

MQTransformer: Multi-Horizon Forecasts with Context Dependent and Feedback-Aware Attention

Carson Eisenach* Yagna Patel† Dhruv Madeka*

July 14, 2021

Abstract

Recent advances in neural forecasting have produced major improvements in accuracy for probabilistic demand prediction. In this work, we propose novel improvements to the current state of the art by incorporating changes inspired by recent advances in Transformer architectures for Natural Language Processing. We develop a novel decoder-encoder attention for context-alignment, improving forecasting accuracy by allowing the network to study its own history based on the context for which it is producing a forecast. We also present a novel positional encoding that allows the neural network to learn context-dependent seasonality functions as well as arbitrary holiday distances. Finally we show that the current state of the art MQ-Forecaster (Wen et al., 2017) models display excess variability by failing to leverage previous errors in the forecast to improve accuracy. We propose a novel decoder-self attention scheme for forecasting that produces significant improvements in the excess variation of the forecast.

1 Introduction

Time series forecasting is a fundamental problem in machine learning with relevance to many application domains including supply chain management, finance, healthcare analytics, and more. Modern forecasting applications require predictions of many correlated time series over multiple horizons. In multi-horizon forecasting, the learning objective is to produce forecasts for multiple future horizons at each time-step. Beyond simple point estimation, decision making problems require a measure of uncertainty about the forecasted quantity. Access to the full distribution is usually unnecessary, and several quantiles are sufficient (many problems in Operations Research use the 50th and 90th percentiles, for example).

As a motivating example, consider a large e-commerce retailer with a system to produce forecasts of the demand distribution for a set of products at a target time T . Using these forecasts as an input, the retailer can then optimize buying and placement decisions to maximize revenue and/or customer value. Accurate forecasts are important, but – perhaps less obviously – forecasts that

*Demand Forecasting, Amazon. Correspondence to: ceisen@amazon.com.

†Work done while at Amazon

don't exhibit excess volatility as a target date approaches minimize costly, bull-whip effects in a supply chain (Chen et al., 2000; Bray and Mendelson, 2012).

Recent work applying deep learning to time-series forecasting focuses primarily on the use of recurrent and convolutional architectures (Nascimento et al., 2019; Yu et al., 2017; Gasparin et al., 2019; Mukhoty et al., 2019; Wen et al., 2017)¹. These are Seq2Seq architectures (Sutskever et al., 2014) – which consist of an *encoder* which takes an input sequence and summarizes it into a fixed-length context vector, and a *decoder* which produces an output sequence. It is well known that Seq2Seq models suffer from an information bottleneck by transmitting information from encoder to decoder via a single hidden state. To address this Bahdanau et al. (2014) introduces a method called *attention*, allowing the decoder to take as input a weighted combination of relevant latent encoder states at each output time step, rather than using a single context to produce all decoder outputs. While NLP is the predominate application of attention architectures, in this paper we show how novel attention modules and positional embeddings can be used to introduce proper inductive biases for probabilistic time-series forecasting to the model architecture.

Even with these shortcomings, this line of work has lead to major advances in forecast accuracy for complex problems, and real-world forecasting systems increasingly rely on neural nets. Accordingly, a need for black-box forecasting system diagnostics has arisen. Stine and Foster (2020b,a) use probabilistic martingales to study the dynamics of forecasts produced by an arbitrary forecasting system. They can be used to detect the degree to which forecasts adhere to the martingale model of forecast evolution (Heath and Jackson, 1994) and to detect unnecessary volatility (above and beyond any inherent uncertainty) in the forecasts produced. Thus, Stine and Foster (2020b,a) describe a way to connect the excess variation of a forecast to accuracy misses against the realized target.

While, multi-horizon forecasting networks such as (Wen et al., 2017; Madeka et al., 2018), minimize quantile loss - the network architectures do not explicitly handle excess variation, since forecasts on any particular date are not made aware of errors in the forecast for previous dates. In short, such tools can be used to detect flaws in forecasts, but the question of how to incorporate that information into model design is unexplored.

Our Contributions

In this paper, we are concerned with both improving forecast accuracy *and* reducing excess forecast volatility. We present a set of novel architectures that seek to remedy some of inductive biases that are currently missing in state of the art MQ-Forecasters (Wen et al., 2017). The major contributions of this paper are

1. **Positional Encoding from Event Indicators:** Current MQ-Forecasters use explicitly engineered holiday “distances” to provide the model with information about the seasonality of the time series. We introduce a novel positional encoding mechanism that allows the network to learn a seasonality function depending on other information of the time series being forecasted, and demonstrate that its a strict generalization of conventional position encoding schemes.

¹For a complete overview see Benidis et al. (2020)

2. **Horizon-Specific Decoder-Encoder Attention:** Wen et al. (2017); Madeka et al. (2018) and other MQ-Forecasters learn a single encoder representation for all future dates and periods being forecasted. We present a novel horizon-specific decoder-encoder attention scheme that allows the network to learn a representation of the past that depends on which period is being forecasted.
3. **Decoder Self-Attention for Forecast Evolution:** To the best of our knowledge, this is *the first work to consider the impacts of network architecture design on forecast evolution*. Importantly, we accomplish this by using attention mechanisms to introduce the right inductive biases, and not by explicitly penalizing a measure of forecast variability. This allows us to maintain a single objective function without needing to make trade-offs between accuracy and volatility.

By providing MQ-Forecasters with the structure necessary to learn *context information dependent encodings*, we observe major increases in accuracy (3.9% in overall P90 quantile loss throughout the year, and up to 60% during peak periods) on our demand forecasting application along with a significant reduction in excess volatility (52% reduction in excess volatility at P50 and 30% at P90). We also apply MQTransformer to two public datasets, electricity load prediction and retail sales prediction, and show parity with the state-of-the-art on the univariate electricity task, and a 10% improvement over the prior state-of-the-art on the retail task.

2 Background and Related Work

2.1 Time Series Forecasting

Formally, the task considered in our work is the high-dimensional regression problem

$$p(y_{t+1,i}, \dots, y_{t+H,i} | \mathbf{y}_{:t,i}, \mathbf{x}_{:t,i}^{(h)}, \mathbf{x}_{:t,i}^{(f)}, \mathbf{x}_i^{(s)}), \quad (1)$$

where $y_{t+s,i}$, $\mathbf{y}_{:t,i}$, $\mathbf{x}_{:t,i}^{(h)}$, $\mathbf{x}_{:t,i}^{(f)}$, $\mathbf{x}_i^{(s)}$ denote future observations of the target time series i , observations of the target time series observed up until time t , the past covariates, known future information, and static covariates, respectively.

For sequence modeling problems, Seq2Seq (Sutskever et al., 2014) is the canonical deep learning framework and although applied this architecture to neural machine translation (NMT) tasks, it has since been adapted to time series forecasting (Nascimento et al., 2019; Yu et al., 2017; Gasparin et al., 2019; Mukhoty et al., 2019; Wen et al., 2017; Salinas et al., 2020; Wen and Torkkola, 2019). The MQ-Forecaster framework (Wen et al., 2017) solves (1) above by treating each series i as a sample from a joint stochastic process and feeding into a neural network which predicts Q quantiles for each horizon. These types of models, however, inherit from the Seq2Seq architecture the limited contextual information available to the decoder as it produces each estimate $y_{t+s,i}^q$, the q^{th} quantile of the distribution of the target at time $t + s$, $y_{t+s,i}$. Seq2Seq models rely on a single encoded context to produce forecasts for all horizons, imposing an information bottleneck and making it difficult for the model to understand long term dependencies.

Our MQTransformer architecture, like other MQ-Forecasters, uses the direct strategy: the model outputs the quantiles of interest directly, rather than the parameters of a distribution from which

samples are to be generated. This has been shown (Wen et al., 2017) to outperform parametric models, like DeepAR (Salinas et al., 2020), on a wide variety of tasks. Recently, Lim et al. (2019) consider an application of attention to multi-horizon forecasting, but their method still produces a single context for all horizons. Furthermore, by using an RNN decoder their models do not enjoy the same scaling properties as MQ-Forecaster models. To the best of our knowledge, our work is the first to devise attention mechanisms for this problem that readily scale.

2.2 Attention Mechanisms

Bahdanau et al. (2014) introduced the concept of an attention mechanism to solve the information bottleneck and sequence alignment problems in Seq2Seq architectures for NMT. Recently, attention has enjoyed success across a diverse range of applications including natural language processing (NLP), computer vision (CV) and time-series forecasting tasks (Galassi et al., 2019; Xu et al., 2015; Shun-Yao Shih and Fan-Keng Sun and Hung-yi Lee, 2019; Kim and Kang, 2019; Cinar et al., 2017; Li et al., 2019; Lim et al., 2019). Many variants have been proposed including self-attention and dot-product attention (Luong et al., 2015; Cheng et al., 2016; Vaswani et al., 2017; Devlin et al., 2019), and transformer architectures (end-to-end attention with no recurrent layers) achieve state-of-the-art performance on most NLP tasks.

Time series forecasting applications exhibit seasonal trends and the absolute position encodings commonly used in the literature cannot be applied. Our work differs from previous work on *relative position encodings* (Dai et al., 2019; Huang et al., 2018; Shaw et al., 2018) in that we learn a representation from a time series of indicator variables which encode events relevant to the target application (such as holidays and promotions). If event indicators relevant to the application are provided, then this imposes a strong inductive bias that will allow the model to generalize well to future observations. Existing encoding schemes either involve feature engineering (e.g. sinusoidal encodings) or have a maximum input sequence length, ours requires no feature engineering – the model learns it directly from raw data – and it extends to arbitrarily long sequences.

In the vanilla transformer (Vaswani et al., 2017), a sinusoidal position embedding is added to the network input and each encoder layer consists of a multi-headed attention block followed by a feed-forward sub-layer. For each head i , the attention score between query q_s and key k_t is defined as follows for the input layer

$$A_{s,t}^h = \mathbf{x}_s^\top \mathbf{W}_q^{h,\top} \mathbf{W}_k^h \mathbf{x}_t + \mathbf{r}_s^\top \mathbf{W}_q^{h,\top} \mathbf{W}_k^h \mathbf{x}_t + \mathbf{x}_s^\top \mathbf{W}_q^{h,\top} \mathbf{W}_k^h \mathbf{r}_t + \mathbf{r}_s^\top \mathbf{W}_q^{h,\top} \mathbf{W}_k^h \mathbf{r}_t \quad (2)$$

where \mathbf{x}_s , \mathbf{r}_s are the observation of the time series and the position encoding, respectively, at time s . Section 3 introduces attention mechanisms that differ in their treatment of the position dependent biases. See Appendix A for additional discussion of attention mechanisms.

2.3 Martingale Diagnostics

Originally the *martingale model of forecast evolution* (MMFE) was conceived as a way to simulate demand forecasts used in inventory planning problems (Heath and Jackson, 1994). Denoting by $\hat{Y}_{T|t}$ the forecast for Y_T made at time $t \leq T$, the MMFE assumes that the forecast process $\{\hat{Y}_{T|t}\}_t$ is

martingale. Informally, a martingale captures the notion that a forecast should use all information available to the forecasting system at time t . Mathematically, a discrete time martingale is a stochastic process $\{X_t\}$ such that

$$\mathbb{E}[X_{t+1}|X_t, \dots, X_1] = X_t.$$

We assume a working knowledge of martingales and direct the reader to Williams (1991) for a thorough coverage in discrete time.

Taleb (2018) describe how martingale forecasts correspond to rational updating, then expanded by Augenblick and Rabin (2019). Taleb (2018), Taleb and Madeka (2019) and Augenblick and Rabin (2019) go on to develop tests for forecasts that rule out martingality and indicate irrational or predictable updating for binary bets. Stine and Foster (2020a,b) further extend these ideas to quantile forecasts. Specifically, they consider the coverage probability process $p_t := \mathbb{P}[Y_T \leq \tau | Y_s, s \leq t] = \mathbb{E}[I(Y_T \leq \tau) | Y_s, s \leq t]$, where τ denotes the forecast announced in the first period $t = 0$. Because $\{p_t\}$ is also a martingale, the authors show that

$$\mathbb{E}[(p_T - \pi)^2] = \sum_{t=1}^T \mathbb{E}[(p_t - p_{t-1})^2] = \pi(1 - \pi),$$

where $\pi = p_0$ is the expected value of p_T , a Bernoulli random variable, across realizations of the coverage process. In the context of quantile forecasting, π is simply the quantile forecasted. The measure of excess volatility proposed is the quadratic variation process associated with $\{p_t\}$, $Q_s := \sum_{t=0}^s (p_t - p_{t-1})^2$. While this process is not a martingale, we do know that under the MMFE assumption, $\mathbb{E}[Q_T] = \pi(1 - \pi)$. A second quantity of interest is the martingale $V_t := Q_t - (p_t - \pi)^2$ which follows the typical structure of subtracting the compensator to turn a sub-martingale into a martingale. In Section 4 we leverage the properties of $\{V_t\}$ and $\{Q_t\}$ to compare the dynamics of forecasts produced by a variety of models, demonstrating that our feedback-aware decoder self-attention units reduce excess forecast volatility.

Notation

We denote by H and Q the number of horizons and quantiles being forecast, respectively. Bolded characters are used to indicate vector and matrix values. The concatenation of two vectors \mathbf{v} and \mathbf{u} is denoted as $[\mathbf{u}; \mathbf{v}]$.

3 Methodology

As mentioned, this work is motivated in part by the needs of the consumers of forecasting systems. We therefore care about whether or not our innovations can be used in practice. Our methodology must scale to forecasting tens of thousands or millions of signals, at hundreds of horizons. We extend the MQ-Forecaster family of models (Wen et al., 2017) because it, unlike many other architectures considered in the literature, can be applied at a large-scale (millions of samples) due to its use of *forking sequences* – a technique to dramatically increase the effective batch size during training and

avoid expensive data augmentation. In this section we present our MQTransformer architecture, building upon the MQ-Forecaster framework.

For ease of exposition, we reformulate the generic probabilistic forecasting problem in (1) as

$$p(y_{t+1,i}, \dots, y_{t+H,i} | \mathbf{y}_{:t,i}, \mathbf{x}_{:t,i}, \mathbf{x}_i^{(l)}, \mathbf{x}^{(g)}, \mathbf{s}_i),$$

where $\mathbf{x}_{:t,i}$ are past observations of all covariates, $\mathbf{x}_i^{(l)} = \{\mathbf{x}_{s,i}^{(l)}\}_{s=1}^{\infty}$ are known covariates specific to time-series i , $\mathbf{x}^{(g)} = \{\mathbf{x}_s^{(g)}\}_{s=1}^{\infty}$ are the global, known covariates. In this setting, known signifies that the model has access to (potentially noisy) observations of past and future values. Note that this formulation is equivalent to (1), and that known covariates can be included in the past covariates $\mathbf{x}_{:t}$. When it can be inferred from context, the time series index i is omitted.

The rest of this section is organized as follows: first we describe the learning objective and high level architecture, followed by details of our position encoding, horizon-specific attention mechanism and our decoder self-attention mechanism.

3.1 Learning Objective

We train a quantile regression model to minimize the quantile loss, summed over all forecast creation dates and quantiles

$$\sum_t \sum_q \sum_k L_q \left(y_{t+k}, \hat{y}_{t+k}^{(q)} \right),$$

where $L_q(y, \hat{y}) = q(y - \hat{y})_+ + (1 - q)(\hat{y} - y)_+$, $(\cdot)_+$ is the positive part operator, q denotes a quantile, and k denotes the horizon.

3.2 Network Architecture

The design of the architecture is similar to MQRNN (Wen et al., 2017), and consists of encoder, decoder and position encoding blocks. The position encoding outputs, for each time step t , are a representation of global position information, $\mathbf{r}_t^{(g)} = \text{PE}_t^{(g)}(\mathbf{x}^{(g)})$, as well as time-series specific context information, $\mathbf{r}_t^{(l)} = \text{PE}_t^{(l)}(\mathbf{x}_i^{(l)})$. Intuitively, $\mathbf{r}_t^{(g)}$ captures position information that is independent of the time-series i (such as holidays), whereas $\mathbf{r}_t^{(l)}$ encodes time-series specific context information (such as promotions). In both cases, the inputs are a time series of indicator variables *and require no feature-engineering or handcrafted functions*.

The encoder then summarizes past observations of the covariates into a sequence of hidden states $\mathbf{h}_t := \text{encoder}(\mathbf{y}_{:t}, \mathbf{x}_{:t}, \mathbf{r}_{:t}^{(g)}, \mathbf{r}_{:t}^{(l)}, \mathbf{s})$. Using these representations, the decoder produces an $H \times Q$ matrix of forecasts $\hat{\mathbf{Y}}_t = \text{decoder}(\mathbf{h}_{:t}, \mathbf{r}^{(g)}, \mathbf{r}^{(l)})$. Note that in the decoder, the model has access to position encodings.

MQTransformer

Now we describe a design, evaluated in Section 4, following the generic pattern given above. We define the combined position encoding as $\mathbf{r} := [\mathbf{r}^{(g)}; \mathbf{r}^{(l)}]$. In the encoder we use a stack of dilated

Table 1: MQTransformer encoder and decoder

ENCODER	DECODER CONTEXTS
$\mathbf{h}_t^1 = \text{TEMPORALCONV}(\mathbf{y}_{:t}, \mathbf{x}_{:t}, \mathbf{r}_{:t})$ (3)	$\mathbf{c}_{t,h}^{hs} = \text{HSATTENTION}(\mathbf{h}_{:t}, \mathbf{r})$ (4)
$\mathbf{h}_t^2 = \text{FEEDFORWARD}(\mathbf{s})$	$\mathbf{c}_t^a = \text{FEEDFORWARD}(\mathbf{h}_t, \mathbf{r})$
$\mathbf{h}_t = [\mathbf{h}_t^1; \mathbf{h}_t^2],$	$\mathbf{c}_t = [\mathbf{c}_{t,1}^a; \dots; \mathbf{c}_{t,H}^{hs}; \mathbf{c}_t^a]$
	$\tilde{\mathbf{c}}_{t,h} = \text{DSATTENTION}(\mathbf{c}_{:t}, \mathbf{h}_{:t}, \mathbf{r}),$

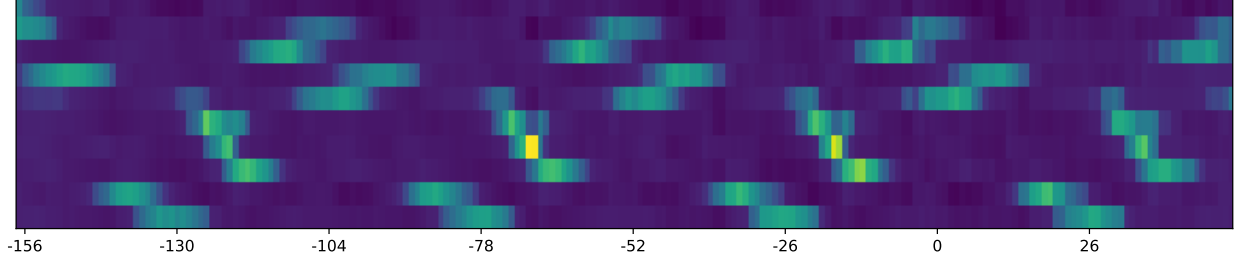


Figure 1: Position encoding learned from daily-grain event indicators

temporal convolutions (van den Oord et al., 2016; Wen et al., 2017) to encode historical time-series and a multi-layer perceptron to encode the static features as (3).

Our decoder incorporates our horizon specific and decoder self-attention blocks, and consists of two branches. The first (global) branch summarizes the encoded representations into horizon-specific ($\mathbf{c}_{t,h}^{hs}$) and horizon agnostic (\mathbf{c}_t^a) contexts. Formally, the global branch $\mathbf{c}_t := m_G(\cdot)$ is given by (4).

The output branch consists of a self-attention block followed by a local MLP, which produces outputs using the same weights for each horizon. For FCT t and horizon h , the output is given by $(\hat{y}_{t+h}^1, \dots, \hat{y}_{t+h}^Q) = m_L(\mathbf{c}_t^a, \mathbf{c}_{t,h}^{hs}, \tilde{\mathbf{c}}_{t,h}, \mathbf{r}_{t+h})$, where $\mathbf{c}_{:t}$ denotes the output of the global branch, up through the FCT t . Next we describe the specifics of our position encoding and attention blocks.

3.3 Learning Position and Context Representations from Event Indicators

Prior work typically uses a variant on one of two approaches to provide attention blocks with position information: (1) a handcrafted representation (such as sinusoidal encodings) or (2) a matrix $\mathbf{M} \in \mathbb{R}^{L \times d}$ of position encoding where L is the maximum sequence length and each row corresponds to the position encoding for time point.

In contrast, our novel encoding scheme maps sequences of indicator variables to a d -dimensional representations. For demand forecasting, this enables our model to learn an arbitrary function of events (like holidays and promotions) to encode position information. As noted above, our model includes two position encodings: $r_t^{(g)} := PE_t^{(g)}(\mathbf{x}^{(g)})$ and $r_t^{(l)} := PE_t^{(l)}(\mathbf{x}^{(l)})$, one that is shared among all time-series i and one that is specific. For the design we use in Section 4, $PE^{(g)}$ is implemented as a bidirectional 1-D convolution and $PE^{(l)}$ is an MLP applied separately at each time

step. Figure 1 shows an example of $PE^{(g)}$ learned from holiday indicator variables. For reference, MQCNN uses linear holiday and promotion distances to represent position information.

Connection to matrix embeddings

Another way to view our position encoding scheme is as a form of set based indexing into rows of an infinite dimensional matrix. We note that the traditional method of learning a matrix embedding \mathbf{M} can be recovered as a special case of our approach. Consider a sequence of length L , and take $\mathbf{x}^{(g)} := [\mathbf{e}_1, \dots, \mathbf{e}_L]$ where \mathbf{e}_s is used to denote the vector in \mathbb{R}^L with a 1 in the s^{th} position and 0s elsewhere. To recover the matrix embedding scheme, we define $PE_t^{\text{matrix}}(\mathbf{x}^{(g)}) := \mathbf{x}_t^{(g), \top} \mathbf{M}$. Thus we see that our scheme is a strict generalization of the matrix embedding approach commonly used in the NLP community.

3.4 Context Dependent and Feedback-Aware Attention

Table 2: Attention weight and output computations for blocks introduced in Section 3.4

BLOCK	ATTENTION WEIGHTS	OUTPUT
DECODER-ENCODER ATTENTION	$A_{t,s}^h = \mathbf{q}_t^{h,\top} \mathbf{W}_q^\top \mathbf{W}_k \mathbf{k}_s \quad (5)$ $\mathbf{q}_t^h = [\mathbf{h}_t; \mathbf{r}_t; \mathbf{r}_{t+h}]$ $\mathbf{k}_s = [\mathbf{h}_s; \mathbf{r}_s]$ $\mathbf{v}_s = \mathbf{h}_s$	$\mathbf{c}_{t,h}^{hs} = \sum_{s=t-L}^t A_{t,s}^h \mathbf{v}_s \quad (6)$
DECODER SELF-ATTENTION	$A_{t,s,r}^h = \mathbf{q}_{t,h}^\top \mathbf{W}_q^{h,\top} \mathbf{W}_k^h \mathbf{k}_{s,r} \quad (7)$ $\mathbf{q}_{t,h} = [\mathbf{h}_t; \mathbf{c}_{t,h}^{hs}; \mathbf{r}_t; \mathbf{r}_{t+h}]$ $\mathbf{k}_{s,r} = [\mathbf{c}_{s,r}^{hs}; \mathbf{r}_s; \mathbf{r}_{s+r}]$ $\mathbf{v}_{s,r} = \mathbf{c}_{s,r}^{hs}$	$\tilde{\mathbf{c}}_{t,h}^{hs} = \sum_{(s,r) \in \mathcal{H}(t,h)} A_{s,t,r}^h \mathbf{v}_{s,r}, \quad (8)$ $\mathcal{H}(t,h) := \{(s,r) s+r = t+h\}$

Horizon-Specific Decoder-Encoder Attention

Our horizon-specific attention mechanism can be viewed as a multi-headed attention mechanism where the projection weights are shared across all horizons. Each head corresponds to a different horizon. In our architecture, the inputs to the block are the encoder hidden states and position encodings. Mathematically, for time s and horizon h , the attention weight for the value at time t is computed as (5).

Observe that there are two key differences between these attention scores and those in the vanilla transformer architecture: (a) projection weights are shared by all H heads, (b) the addition of the position encoding of the target horizon h to the query. The output of our horizon specific

decoder-encoder attention block, $\mathbf{c}_{t,h}^{hs}$, is obtained by taking a weighted sum of the encoder hidden contexts, up to a maximum look-back of L periods as in (6).

Decoder Self-Attention

The martingale diagnostic tools developed in (Stine and Foster, 2020b) indicate a deep connection between accuracy and volatility. We leverage this connection to develop a novel decoder self-attention scheme for multi-horizon forecasting. To motivate the development, consider a model which forecasts values of 40, 60 when the demand has constantly been 50 units. We would consider this model to have excess volatility. Similarly, a model forecasting 40, 60 when demand jumps between 40 and 60 units would not be considered to have excess volatility. This is because the first model fails to learn from its past forecasts - it continues jumping between 40, 60 when the demand is 50 units.

In order to ameliorate this, we need to pass the information of the previous forecast errors into the current forecast. For each FCT t and horizon h , the model attends on the previous forecasts using a query containing the demand information for that period. The attention mechanism has a separate head for each horizon.

Rather than attend on the demand information and prior outputs directly, a richer representations of the same information is used: the demand information at time t is incorporated via the encoded context \mathbf{h}_t and previous forecasts are represented via the corresponding horizon-specific context $\mathbf{c}_{s,r}^{hs}$ – in the absence of decoder-self attention $\mathbf{c}_{s,r}^{hs}$ would be passed through the local MLP to generate the forecasts. Formally, the attention scores are given by (7). The horizon-specific and feedback-aware outputs, $\tilde{\mathbf{c}}_{t,h}^{hs}$, are given by (8). Note how we sum only over previous forecasts of the same period.

4 Empirical Results

4.1 Large-Scale Demand Forecasting

First, we evaluate our architecture on a demand forecasting problem for a large-scale e-commerce retailer with the objective of producing multi-horizon forecasts that span up to one year. Each horizon is specified by a lead time (LT), number of periods from the FCT to the start of the horizon, and a span (SP), number of periods covered by the forecast, combination. To assess the effects of each innovation, we ablate by removing components one at a time. MQTransformer is denoted as **Dec-Enc & Dec-Self Att**, **Dec-Enc Att** – which contains only the horizon-specific decoder-encoder unit – and **Baseline** – the vanilla MQCNN model.

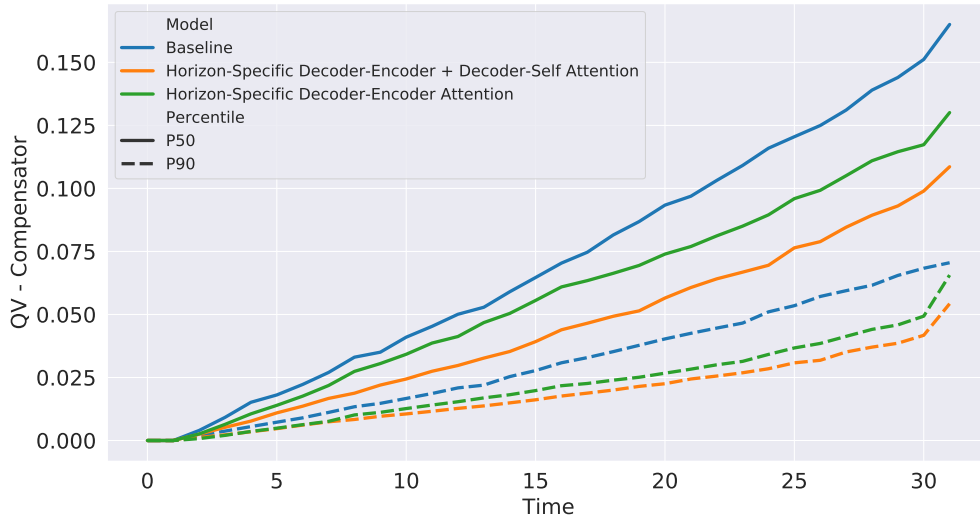
We conduct our experiments on a subset of products (~ 2 million products) in the US store. Each model is trained using a single machine with 8 NVIDIA V100 Tensor Core GPUs, on three years of demand data (2015-2018); one year (2018-2019) is held out for back-testing.

Forecast Accuracy

Table 3 summarizes several key metrics that demonstrate the accuracy improvements achieved by adding our proposed attention mechanisms to the MQCNN architecture – the full set of results can be found in Appendix B. Introducing the Horizon-Specific Decoder-Encoder attention alone yields

Table 3: Aggregate Quantile Loss Metrics

MODEL	ALL LTSP	LTSP 0/4	SEASONAL PEAK 1	POST-PEAK RAMPDOWN	PROMOTION TYPE 1
BASELINE	1.000	1.000	1.000	1.000	1.000
DEC-ENC	0.984	0.931	0.748	0.712	0.706
DEC-ENC + DEC-SELF	0.989	0.908	0.698	0.639	0.670

Figure 2: Martingale diagnostic process $\{V_t\}$ averaged over all weeks in test period (2018-2019)

improvements along all metrics evaluated. Overall we see a 1.6% improvement in P50 QL and a 3.9% improvement in P90 QL. Notably, the attention mechanism yields significant improvements on short LTSP (LTSP 0/4).

Further, Table 3 demonstrates improved performance on seasonal peaks and promotions. Observe that while MQCNN performs well on some seasonal peaks, it also is misaligned and fails to ramp-down post-peak – post-peak ramp-down issues occur when the model continues to forecast high for target weeks after the peak week. By including MQTransformer’s attention mechanisms in the architecture, we see a 43% improvement for Seasonal Peak 1 and a 56% improvement on Post-Peak Rampdown. In retail, promotions are used to provide a demand lift for products. Accordingly, a model should be able to react to the upcoming promotion and forecast an accurate lift in demand for the target weeks in which the promotion is placed. From Table 3 we see that MQTransformer achieves a 49% on items with Promotion Type 1 versus the baseline.

Forecast Volatility

We study the effect of our proposed attention mechanisms on excess forecast volatility using diagnostic tools recently proposed by [Stine and Foster \(2020b,a\)](#). Figure 2 plots the process $\{V_t\}$ (see Section 2). In the plot, the lines should appear horizontal under the MMFE. Any deviation above this (on an aggregate level) indicates excess volatility in the forecast evolution. We can observe that while none of the models produce ideal forecasts, both attention models outperform the Baseline with the attention model with both proposed attention mechanisms performing the best in terms of these evolution diagnostics.

The green line corresponds to the attention model with only the horizon-specific decoder-encoder attention. We can see that compared to the baseline, this model achieves up to 27% reduction in excess volatility at P50 and 7% at P90. By also adding decoder-self attention we see a further reduction in excess volatility of an additional 20% at P50 and 21% at P90.

4.2 Publicly Available Datasets

Following [Lim et al. \(2019\)](#), we consider applications to brick-and-mortar retail sales forecasting and electricity load prediction. For the retail task, we predict the next 30 days of sales, given the previous 90 days of history. This dataset contains a rich set of static, time series, and known features. At the other end of the spectrum, the electricity load dataset is univariate. Table 4 compares MQTransformer’s performance with other recent works² – DeepAR ([Salinas et al., 2020](#)), ConvTrans ([Li et al., 2019](#)), MQRNN ([Wen et al., 2017](#)), and TFT ([Lim et al., 2019](#)).

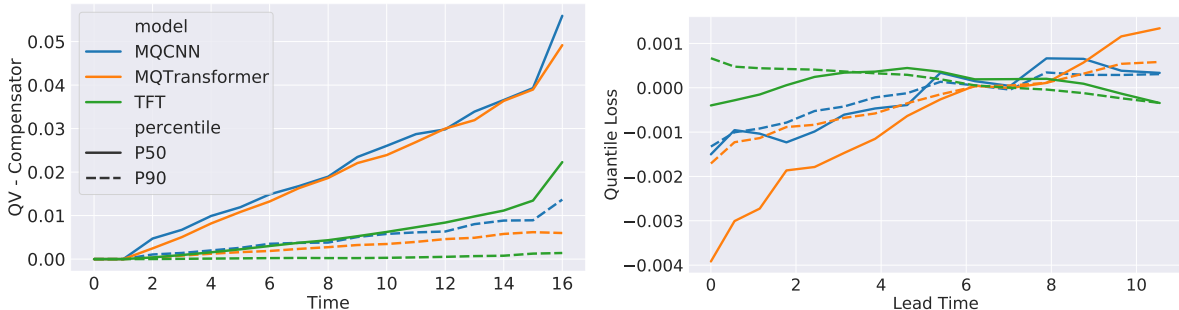


Figure 3: Forecast evolution analysis on Favorita dataset. Left: Martingale Diagnostic Process $\{V_t\}$. Right: QL by lead time, averaged over target dates from 2016-03-01 through 2016-05-01; QL trajectories are centered around 0.

Our MQTransformer architecture is competitive with the state-of-the-art on the electricity load prediction task, but on the task with richer information, it dramatically outperforms all other models as shown in Figure 4. On the Favorita retail forecasting task, Figure 3 shows that as expected, MQTransformer substantially reduces excess volatility in the forecast evolution. Somewhat

²All results except MQTransformer are from [Lim et al. \(2019\)](#), we used their pre-processing and evaluation code to ensure parity

surprisingly, TFT exhibits much lower volatility than does MQTransformer. In Figure 3, the right hand plot displays quantile loss as the target date approaches – trajectories for each model are zero centered to emphasize the trends exhibited. While TFT is less volatile, *it is also less accurate* as it fails to incorporate newly available information. By contrast, MQTransformer is both *less volatile* and *more accurate* when compared with MQCNN. Additional details regarding the experimental setup and datasets can be found in Appendix C.

Table 4: P50 and P90 QL on electricity and retail datasets with the best results on each task emphasized

TASK	MODEL									
	DEEPAR		CONVTRANS		MQRNN		TFT		MQTRANSFORMER	
	P50	P90	P50	P90	P50	P90	P50	P90	P50	P90
ELEC.	0.075	0.040	0.059	0.034	0.077	0.036	0.055	0.027	0.057	0.027
RETAIL	0.574	0.230	0.429	0.192	0.379	0.152	0.354	0.147	0.323	0.133

5 Conclusions and Future Work

In this work, we present three novel architecture enhancements that improve bottlenecks in state of the art MQ-Forecasters. We presented a series of architectural innovations for probabilistic time-series forecasting including a novel alignment decoder-encoder attention, as well as a decoder self-attention scheme tailored to the problem of multi-horizon forecasting. To the best of our knowledge, this is the first work to consider the impact of model architecture on forecast evolution. We also demonstrated how position embeddings can be learned directly from domain-specific event indicators and horizon-specific contexts can improve performance for difficult sub-problems such as promotions or seasonal peaks. Together, these innovations produced significant improvements in the excess variation of the forecast and accuracy across different dimensions. Finally, we applied our model to several public datasets, where it beat the previous state-of-the-art by 10% on the more complex task. An interesting direction we intend to explore in future work is incorporating encoder self-attention so that the model can leverage arbitrarily long historical time series, rather than the fixed length consumed by the convolution encoder.

Acknowledgements

We would like to thank Dean Foster, Robert Stine, and Kari Torkkola for their insightful feedback and support.

References

- AUGENBLICK, N. and RABIN, M. (2019). Belief movement, uncertainty reduction, and rational updating. Tech. rep., Haas School of Business, University of California, Berkeley.
- BAHDANAU, D., CHO, K. and BENGIO, Y. (2014). Neural machine translation by jointly learning to align and translate. [arXiv:1409.0473](#).
- BENIDIS, K., RANGAPURAM, S. S., FLUNKERT, V., WANG, B., MADDIX, D., TURKMEN, C., GASTHAUS, J., BOHLKE-SCHNEIDER, M., SALINAS, D., STELLA, L. ET AL. (2020). Neural forecasting: Introduction and literature overview. [arXiv:2004.10240](#).
- BRAY, R. L. and MENDELSON, H. (2012). Information Transmission and the Bullwhip Effect: An Empirical Investigation. *Management Science* **58** 860–875.
- CHEN, F., DREZNER, Z., RYAN, J. K. and SIMCHI-LEVI, D. (2000). Quantifying the Bullwhip Effect in a Simple Supply Chain: The Impact of Forecasting, Lead Times, and Information. *Management Science* **46** 436–443.
- CHENG, J., DONG, L. and LAPATA, M. (2016). Long short-term memory-networks for machine reading. [arXiv:1601.06733](#).
- CINAR, Y. G., MIRISAEI, H., GOSWAMI, P., GAUSSIER, E., AIT-BACHIR, A. and STRIJOV, V. (2017). Position-based content attention for time series forecasting with sequence-to-sequence rnns. In *ICONIP*.
- DAI, Z., YANG, Z., YANG, Y., CARBONELL, J., LE, Q. V. and SALAKHUTDINOV, R. (2019). Transformer-XL: Attentive Language Models Beyond a Fixed-Length Context. In *ACL*.
- DEVLIN, J., CHANG, M.-W., LEE, K. and TOUTANOVA, K. (2019). BERT: Pre-training of Deep Bidirectional Transformers for Language Understanding. In *NAACL-HLT*.
- GALASSI, A., LIPPI, M. and TORRONI, P. (2019). Attention, please! a critical review of neural attention models in natural language processing. [arXiv:1902.02181](#).
- GASPARIN, A., LUKOVIC, S. and ALIPPI, C. (2019). Deep Learning for Time Series Forecasting: The Electric Load Case. [arXiv:1907.09207](#).
- HEATH, D. C. and JACKSON, P. L. (1994). Modeling the evolution of demand forecasts with application to safety stock analysis in production/distribution systems. *IIE transactions* **26** 17–30.
- HUANG, C.-Z. A., VASWANI, A., USZKOREIT, J., SHAZEER, N., SIMON, I., HAWTHORNE, C., DAI, A. M., HOFFMAN, M. D., DINCULESCU, M. and ECK, D. (2018). Music Transformer: Generating Music with Long-Term Structure. [arXiv:1809.04281](#).
- KIM, S. and KANG, M. (2019). Financial series prediction using Attention LSTM. [arXiv:1902.10877](#).

- LI, S., JIN, X., XUAN, Y., ZHOU, X., CHEN, W., WANG, Y.-X. and YAN., X. (2019). Enhancing the locality and breaking the memory bottleneck of transformer on time series forecasting. In *NIPS*.
- LIM, B., ARIK, S. O., LOEFF, N. and PFISTER, T. (2019). Temporal Fusion Transformers for Interpretable Multi-horizon Time Series Forecasting. [arXiv:1912.09363](#).
- LUONG, M.-T., PHAM, H. and MANNING, C. D. (2015). Effective approaches to attention-based neural machine translation. [arXiv:1508.04025](#).
- MADEKA, D., SWINIARSKI, L., FOSTER, D., RAZOUMOV, L., TORKKOLA, K. and WEN, R. (2018). Sample path generation for probabilistic demand forecasting. In *ICML workshop on Theoretical Foundations and Applications of Deep Generative Models*.
- MUKHOTY, B. P., MAURYA, V. and SHUKLA, S. K. (2019). Sequence to sequence deep learning models for solar irradiation forecasting. In *IEEE Milan PowerTech*.
- NASCIMENTO, R. C., SOUTO, Y. M., OGASAWARA, E., PORTO, F. and BEZERRA, E. (2019). STConvS2S: Spatiotemporal Convolutional Sequence to Sequence Network for weather forecasting. [arXiv:1912.00134](#).
- SALINAS, D., FLUNKERT, V., GASTHAUS, J. and JANUSCHOWSKI, T. (2020). Deepar: Probabilistic forecasting with autoregressive recurrent networks. *International Journal of Forecasting* **36** 1181–1191.
- SHAW, P., USZKOREIT, J. and VASWANI, A. (2018). Self-Attention with Relative Position Representations. In *NAACL*.
- SHUN-YAO SHIH AND FAN-KENG SUN AND HUNG-YI LEE (2019). Temporal pattern attention for multivariate time series forecasting. *Machine Learning* **108** 1421–1441.
- STINE, R. and FOSTER, D. (2020a). Martingale Descriptions of the Evolution of Forecasts. Tech. rep., Manuscript in preparation.
- STINE, R. and FOSTER, D. (2020b). Martingale Diagnostics. Tech. rep., Manuscript in preparation.
- SUTSKEVER, I., VINYALS, O. and LE, Q. V. (2014). Sequence to sequence learning with neural networks. In *NIPS*.
- TALEB, N. N. (2018). Election predictions as martingales: an arbitrage approach. *Quantitative Finance* **18** 1–5.
- TALEB, N. N. and MADEKA, D. (2019). All roads lead to quantitative finance. *Quantitative Finance* **19** 1775–1776.
- VAN DEN OORD, A., DIELEMAN, S., ZEN, H., SIMONYAN, K., VINYALS, O., GRAVES, A., KALCHBRENNER, N., SENIOR, A. and KAVUKCUOGLU, K. (2016). Wavenet: A generative model for raw audio. [arXiv:1609.03499](#).

- VASWANI, A., SHAZEER, N., PARMAR, N., USZKOREIT, J., JONES, L., GOMEZ, A. N., KAISER, L., and POLOSUKHIN, I. (2017). Attention is all you need. In *NIPS*.
- WEN, R. and TORKKOLA, K. (2019). Deep Generative Quantile-Copula Models for Probabilistic Forecasting. In *ICML Time Series Workshop*.
- WEN, R., TORKKOLA, K., NARAYANASWAMY, B. and MADEKA, D. (2017). A multi-horizon quantile recurrent forecaster. In *NIPS Time Series Workshop*.
- WILLIAMS, D. (1991). *Probability with Martingales*. Cambridge University Press.
- XU, K., BA, J., KIROS, R., CHO, K., COURVILLE, A., SALAKHUDINOV, R., ZEMEL, R. and BENGIO, Y. (2015). Show, attend and tell: Neural image caption generation with visual attention. In *ICML*.
- YU, R., ZHENG, S., ANANDKUMAR, A. and YUE, Y. (2017). Long-term Forecasting using Higher Order Tensor RNNs. [arXiv:1711.00073](https://arxiv.org/abs/1711.00073).

A Additional Background and Related Work

A.1 Attention Mechanisms

Attention mechanisms can be viewed as a form of content based addressing, that computes an alignment between a set of *queries* and *keys* to extract a *value*. Formally, let $\mathbf{q}_1, \dots, \mathbf{q}_t, \mathbf{k}_1, \dots, \mathbf{k}_t$ and $\mathbf{v}_1, \dots, \mathbf{v}_t$ be a series of queries, keys and values, respectively. The s^{th} attended value is defined as $\mathbf{c}_s = \sum_{i=1}^t \text{score}(\mathbf{q}_s, \mathbf{k}_i) \mathbf{v}_i$, where score is a scoring function – commonly $\text{score}(\mathbf{u}, \mathbf{v}) := \mathbf{u}^\top \mathbf{v}$. In the vanilla transformer model, $\mathbf{q}_s = \mathbf{k}_s = \mathbf{v}_s = \mathbf{h}_s$, where \mathbf{h}_s is the hidden state at time s . Because attention mechanisms have no concept of absolute or relative position, some sort of position information must be provided. Vaswani et al. (2017) uses a sinusoidal positional encoding added to the input to an attention block, providing each token’s position in the input time series.

B Additional Results: Large Scale Demand Forecasting

Tables 5, 6, and 7 contain the full set of results on the large scale demand forecasting task. We were unable to compare to TFT (the prior state of the art on several public datasets) as it does not scale-up, however we anticipate it would not have performed as well as MQTransformer (or even MQCNN) as it relies heavily on item-specific embeddings and the pre-processing in Lim et al. (2019) filters all items not seen in the training period from the test set.

Quantile loss by horizon

Table 5 demonstrates how the attention mechanism yields significant improvements in shorter LTSP (e.g. LTSP 3/1 and LTSP 0/4), 7% improvement in P90 QL for LTSP 3/1 and 7.6% improvement in P90 QL for LTSP 0/4. We still see improvements for longer LTSP, but they are less substantial: 3.8% improvement in P90 QL for LTSP 12/3 and 3.9% improvement in P90 QL for LTSP 0/33. By also adding decoder-self attention, we continue to see improved results for shorter LTSP compared to only decoder-encoder attention, but we do see slight degradations for longer LTSP when comparing to decoder-encoder attention.

Promotions Performance

In Table 7 we see that MQTransformer outperforms the prior state of the art on all promotion types. After adding the horizon-specific decoder-encoder and decoder-self attentions, versus the baseline, we see a 49% improvement for Promotion Type 1 products, a 31% improvement for Promotion Type 2 products, and a 17% improvement for Promotion Type 3 products.

Peak Performance

Table 3 illustrates that while MQCNN performs well on some seasonal peaks, it also is misaligned and fails to rampdown post-peak – ramp-down issues occur when the model continues to forecast high for target weeks after the peak week. By including MQTransformer’s attention mechanisms in

the architecture, we see a 43% improvement for Seasonal Peak 1, a 21% improvement for Seasonal Peak 2, a 7% improvement for Seasonal Peak 3, and a 56% improvement on Post-Peak Rampdown.

Table 5: 52-week aggregate quantile loss metrics with for a set of representative lead times and spans

MODEL	ALL LTSP		LTSP 3/1		LTSP 0/4	
	P50	P90	P50	P90	P50	P90
BASILINE	1.000	1.000	1.000	1.000	1.000	1.000
DEC-ENC	0.984	0.960	0.950	0.927	0.963	0.931
DEC-ENC & DEC-SELF	0.989	0.984	0.934	0.911	0.948	0.908

MODEL	LTSP 12/3		LTSP 0/33	
	P50	P90	P50	P90
BASILINE	1.000	1.000	1.000	1.000
DEC-ENC	0.975	0.957	0.982	0.963
DEC-ENC & DEC-SELF	0.960	0.964	0.982	0.981

Table 6: P90 quantile loss metrics on seasonal peak target weeks

MODEL	SEASONAL	SEASONAL	SEASONAL	POST-PEAK
	PEAK 1	PEAK 2	PEAK 3	RAMPDOWN
BASILINE	1.000	1.000	1.000	1.000
DEC-ENC	0.748	0.817	0.962	0.712
DEC-ENC + DEC-SELF	0.698	0.826	0.931	0.639

C Experiments on Public Datasets

For both tasks we used the architecture described in Section 3 with a hidden layer size of 128 (where relevant). We use a stack of 5 dilated temporal convolutions for the position encodings and the wave-net encoder in both tasks, giving it a field of view of 24 and 30 time steps on the electricity and retail tasks, respectively. On the retail task we used attention units with 30 heads (one for each horizon) with a per-head dimension of 20. Our pre-processing methodology is identical to that used by Lim et al. (2019) – to ensure a fair comparison – with one exception: we do not not normalize inputs to our model. This datasets and the preprocessing applied are described below.

Table 7: P90 quantile loss metrics on item, weeks with promotions

MODEL	PROMOTION TYPE 1	PROMOTION TYPE 2	PROMOTION TYPE 3
BASELINE	1.000	1.000	1.000
DEC-ENC	0.706	0.769	0.865
DEC-ENC + DEC-SELF	0.670	0.763	0.851

Retail

This dataset is provided by the Favorita Corporacion (a major Grocery chain in Ecuador) as part of a Kaggle³ to predict sales for thousands of items at multiple brick-and-mortar locations. In total there are 135K items (item, store combinations are treated as distinct entities), and the dataset contains a variety of features including: local, regional and national holidays; static features about each item; total sales volume at each location. The task is to predict log-sales for each (item, store) combination over the next 30 days, using the previous 90 days of history. The training period is January 1, 2015 through December 1, 2015. The following 30 days are used as a validation set, and the 30 days after that as the test set. As part of pre-processing, 450K samples are extracted from the histories during the train window. These 30 day windows correspond to a single forecast creation time.

For the volatility analysis presented in Figure 3, we used a 60 day validation window (March 1, 2016 through May 1, 2016), which corresponds to 30 forecast creation times.

Electricity

This dataset consists of time series for 370 customers of at an hourly grain. The univariate data is augmented with a day-of-week, hour-of-day and offset from a fixed time point. The task is to predict hourly load over the next 24 hours for each customer, given the past seven days of usage. From the training period (January 1, 2014 through September, 1 2019) 500K samples are extracted.

³The original competition can be found [here](#).

D Additional Architecture Details

Figure 4 shows a diagram of the MQTransformer architecture.

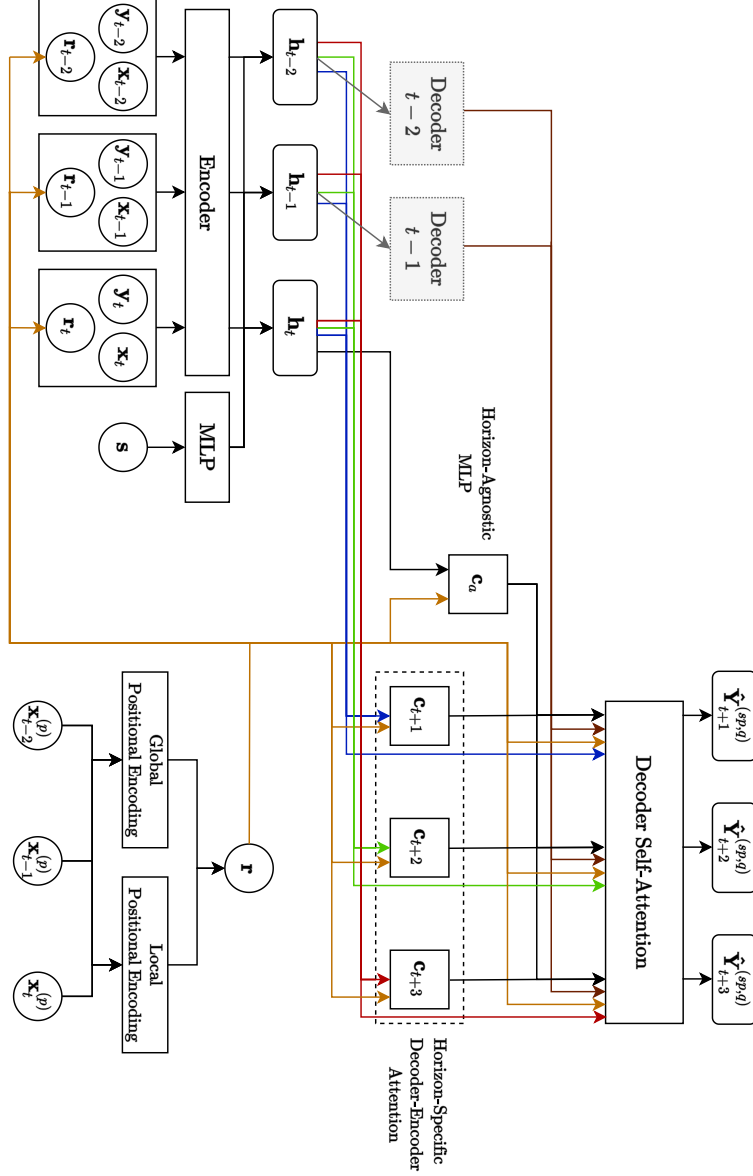


Figure 4: MQTransformer architecture with learned global/local positional encoding, horizon-specific decoder-encoder attention, and decoder self-attention